ELSEVIER

Journal of Molecular Structure 605 (2002) 17–26

Journal of
MOLECULAR
STRUCTURE

www.elsevier.com/locate/molstruc

Proton transfer and coordination properties of aromatic α-hydroxy hydrazones

G.A. Ibañez, G.M. Escandar*, A.C. Olivieri

Departamento de Química Analítica, Facultad de Ciencias Bioquímicas y Farmacéuticas, Universidad Nacional de Rosario, Suipacha 531, Rosario S2002LRK, Argentina

Received 18 April 2001; accepted 8 May 2001

Abstract

The prototropic properties of two nitro derivatives of aromatic α-hydroxy hydrazones [2,4-dinitro-*N*-phenyl-*N*′(2-hydroxy-1-phenylmethylene hydrazine) and 2,4-dinitro-*N*-phenyl-*N*′(2-hydroxy-1-naphthylmethylene hydrazine] have been analysed through electronic absorption, ^{1}H and ^{13}C NMR and semiempirical molecular orbital methods. The metal binding properties of both compounds and of the unsubstituted hydrazones were evaluated from potentiometric and spectrophotometric data in dioxane–water mixtures. On the basis of the spectral analysis and PM3 semiempirical calculations, the structures of the formed complexes were proposed. © 2002 Elsevier Science B.V. All rights reserved.

Keywords: Spectroscopy and potentiometry; Proton transfer; Coordination chemistry; Aromatic α-hydroxy hydrazones

1. Introduction

Specifically for the identification of carbonylic compounds, hydrazones are extensively used in both synthetic and analytical chemistry. They are also employed in the polymer industry (as plasticising agents, antioxidants and polymerisation initiators) and also in the pharmaceutical industry [1,2]. It should be mentioned that certain hydrazones and their copper(II) complexes present biological activity as antitumor agents [3].

In the present work, we continue with the evaluation of aromatic α-hydroxy hydrazones as part of a general program committed to the study of tautomeric and metal binding properties of compounds containing enol–azo or keto–hydrazo functional groups [4–8], with emphasis on the influence of different substituents. Specifically, the analysis of the complexes formed between divalent metal ions and *N*-phenyl-*N*′(2-hydroxy-1-phenylmethylene hydrazine) (PHPH) is carried out. The relationship between the chelating behaviour and the prototropic properties of this compound is assessed. In addition, two nitro derivatives, 2,4-dinitro-*N*-phenyl-*N*′(2-hydroxy-1-phenylmethylene hydrazine) (2,4$(NO_2)_2$PHPH) and 2,4-dinitro-*N*-phenyl-*N*′(2-hydroxy-1-naphthylmethylene hydrazine) (2,4$(NO_2)_2$PHNH) were synthesised, studied and compared with the corresponding unsubstituted substrates. The studies were performed by a combination of electronic absorption, NMR, potentiometry and semiempirical calculations.

---

* Corresponding author. Tel./fax: +54-341-4372-704.
E-mail address: gescanda@fbioyf.unr.edu.ar (G.M. Escandar).

PII: S0022-2860(01)00668-8

2. Experimental

2.1. Reagents and solvents

Stock solutions ca. 0.01 M of Cu(II), Co(II) and Ni(II) were prepared by dissolving the corresponding nitrates (AR) in doubly distilled water. The exact metal concentrations were determined by titrations with previously standardised ethylenediaminetetraacetic acid solution in the presence of appropriate indicators [9]. Solutions of carbonate-free NaOH in 30% dioxane–70% water (v/v) and 70% dioxane–30% water (v/v) were standardised with the use of Gran's plots [10]. Aqueous solutions of carbonate-free NaOH and HNO_3 were standardised against potassium hydrogenphtalate and sodium carbonate, respectively. 1,4 Dioxane (p.a.) was obtained from Merck. The water employed was purified by ion exchange and distilled.

2.2. Synthesis of the ligands

The ligands were prepared using standard procedures [11]. PHPH was prepared as previously described [5]. $2,4(NO_2)_2$PHPH and $2,4(NO_2)_2$PHNH were prepared according to the following procedure: to a clear solution obtained by warming 2,4-phenylhydrazine with concentrated HCl and ethanol, the corresponding ethanolic aldehyde solution (salicylaldehyde or 2-hydroxynaphtalene-1-carbaldehyde) was added. The mixture was heated to just the boiling point and shaken. After cooling, the solid obtained was recrystallised from acetone–ethanol and acetone, respectively. Elemental analyses were performed by Atlantic Microlab Inc., and were in agreement with the calculated values: for PHPH, found: C: 73.54, H: 5.73, N: 13.06%; $C_{13}H_{12}N_2O$ requires: C: 73.56, H: 5.70, N: 13.20%; for $2,4(NO_2)_2$PHPH, found: C: 51.79, H: 3.49, N: 18.56%; $C_{13}H_{10}N_4O_5$ requires: C: 51.61, H: 3.33, N: 18.53%; for $2,4\text{-}(NO_2)_2$–PHNH, found: C: 57.99, H: 3.45, N: 15.88, $C_{17}H_{12}N_4O_5$ requires: C: 59.91, H: 3.41, N: 15.90%. The purity of the ligands was also checked by thin-layer chromatography using different solvent systems and by ^{1}H NMR.

2.3. NMR measurements

Both ^{1}H and ^{13}C NMR spectra for $2,4(NO_2)_2$PHPH were performed on a Brucker AC-200 NMR spectrometer operating at nominal frequencies of 200.1 and 50.3 MHz, respectively, while the corresponding spectra for $2,4(NO_2)_2$PHNH were recorded on a Brucker AM-500 spectrometer operating at nominal frequencies of 500.1 and 125.8 MHz.

2.4. MO calculations

Semiempirical MO calculations in the ground states (geometry optimisation and calculation of heats of formation) of the structures of the compounds and their metal complexes were performed using PM3 [12], as implemented in either the HyperChem 5.02 or Spartan packages of programs on a Pentium II 650 microcomputer. Calculations in the excited states for the nitro derivatives, which are relevant to interpret luminescent properties, were not be performed because the fluorescence emission of these compound is negligible.

2.5. Determination of equilibrium constants

All measurements were carried out at an ionic strength (μ) of 0.10 M ($NaNO_3$) and at a temperature of 20.0°C. Due to the low aqueous solubility of both the compounds under study and their complexes, the determination of the equilibrium constants was carried out in dioxane–water mixtures. The effect of the solvent composition in the pH measurements was taken into account by correcting each metre reading with a conversion factor [13]. This factor was obtained, prior to each experiment, by titration of both 30% v/v and 70% v/v dioxane–water solutions of standard HNO_3 with successive amounts of standard NaOH in the corresponding solvent mixture. In these latter titrations, μ was also adjusted to 0.10 M with $NaNO_3$ and the temperature was maintained at 20.0°C. The log of the water hydrolysis constant values, in our conditions of μ and temperature were found to be -14.2 and -15.5 for 30 and 70% v/v dioxane–water, respectively. The latter value is in accordance with that reported for Motekaitis et al. at 25°C and $\mu = 0.10$ M ($\log K_w = -16$, Ref. [14]). The hydrolysis constant values for the metal ions were obtained from Ref. [15].

2.5.1. Potentiometric determinations

A Metrohm 713 pH meter fitted with glass and

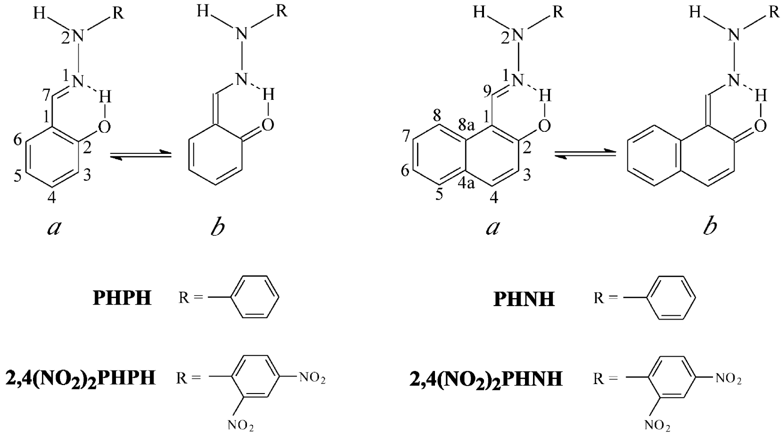

Scheme 1.

reference electrodes was used for the potentiometric measurements. In order to read the hydrogen ion concentration, the electrode was calibrated with buffers at the same μ to that employed in the equilibrium constant determinations. Measurements were made under nitrogen atmosphere in the appropriate dioxane–water mixture. The initial concentrations of ligand and metal were in the range 8.00×10^{-4}–1.00×10^{-3} M. Each run was performed at least in duplicate. The data processing for the computation of the equilibrium constants and of the species distribution diagram were performed using the BEST program [16].

2.5.2. Spectrophotometric determinations

The measurements were made using a Beckman DU640 specrophotometer in 1.00 cm quartz microcells. Conformity to Beer's law in the range of the concentrations used was verified prior to the determinations. The initial concentrations of ligand and metal ion were in the range 1×10^{-5}–1×10^{-4} M. A typical spectrophotometric titration experiment was previously described in the literature [6]. The data were converted into deprotonation constants or equilibrium complex constants with the use of the program STAR [17].

3. Results and discussion

3.1. Structural analysis of the protonated forms

In a previous work, the existence of ground state proton transfer in both PHPH and PHNH was described [7]. With the purpose of investigating this process in the ground state of both $2,4(NO_2)_2$PHPH and $2,4(NO_2)_2$PHNH (Scheme 1), we have studied their prototropic properties and compared them with those for the unsubstituted α-hydroxy hydrazones.

NMR is widely recognised as a highly diagnostic tool for the position of tautomeric equilibria [18,19]. The ^{1}H NMR spectra of $2,4(NO_2)_2$PHPH and $2,4(NO_2)_2$PHNH show the expected complex patterns arising from the many aromatic protons. In the case of $2,4(NO_2)_2$PHPH, a signal ascribed to the labile OH proton was detected at 10.0 ppm. This was not possible for $2,4(NO_2)_2$PHNH, whose spectrum had to be recorded in DMSO due to solubility restrictions. As has been demonstrated [18,19], the ^{13}C NMR chemical shift of the C(2)–O carbon is highly sensitive to the tautomeric structure, with extreme values of ca. 155 ppm in form *a* and ca. 180 ppm in form *b*. The values obtained for $2,4(NO_2)_2$PHPH and $2,4(NO_2)_2$PHNH, 160.6 and 162.9 ppm, respectively, clearly indicate that form *a* is the dominating species in both cases. These results are in agreement with those reported for PHPH (156.9 ppm) and PHNH (156.2 ppm) [7].

The electronic absorption spectra of $2,4(NO_2)_2$PHPH and $2,4(NO_2)_2$PHNH in both chloroform (with maxima at 381 and 410 nm, respectively) and in dioxane–water 70–30% v/v at acid pH (with maxima at 393 and 415 nm, respectively) indicate that both compounds exist primarily in the enol *a* form

Table 1
Relevant PM3 results for the protonated compounds (bond lengths are in Å)

Parameter	PHPH		PHNH		$2,4(NO_2)_2PHPH$		$2,4(NO_2)_2PHNH$	
	a	*b*	*a*	*b*	*a*	*b*	*a*	*b*
ΔH_f^0 (kJ mol^{-1})	177.4	269.5	247.9	289.5	114.5	189.4	184.0	236.9
N–N–C–C–C–O portion								
N–N	1.396	1.365	1.410	1.458	1.399	1.456	1.401	1.457
N–C(7,9)	1.304	1.377	1.306	1.399	1.306	1.407	1.308	1.412
C(7,9)–C(1)	1.460	1.379	1.457	1.370	1.457	1.367	1.453	1.364
C(1)–C(2)	1.412	1.467	1.395	1.474	1.412	1.478	1.397	1.480
C(2)–O	1.356	1.249	1.352	1.235	1.356	1.235	1.352	1.233
Aromatic ring bearing the oxygen								
C(2)–C(3)	1.410	1.467	1.430	1.472	1.410	1.469	1.431	1.471
C(3)–C(4)	1.382	1.350	1.361	1.341	1.382	1.346	1.361	1.341
C(4)–C(5)	1.397	1.439			1.399	1.441		
C(5)–C(6)	1.383	1.354			1.382	1.348		
C(6)–C(1)	1.403	1.445			1.405	1.448		
C(4)–C(4a)			1.425	1.449			1.426	1.450
C(4a)–C(8a)			1.410	1.406			1.410	1.406
C(8a)–C(1)			1.435	1.458			1.437	1.461
Adjacent aromatic ring								
C(4a)–C(5)			1.418	1.402			1.418	1.401
C(5)–C(6)			1.370	1.384			1.371	1.385
C(6)–C(7)			1.411	1.395			1.410	1.395
C(7)–C(8)			1.370	1.384			1.371	1.385
C(8)–C(8a)			1.421	1.404			1.420	1.403

[20]. These results are in agreement with the NMR data discussed above, and also with those found for related unsubstituted hydrazones [5].

Semiempirical MO calculations carried out with the program PM3 (Table 1) are also in agreement with the spectroscopic findings. For comparison, Table 1 lists heats of formation and relevant bond distances for the studied dinitro derivatives and also for the parent compounds PHPH and PHNH. As can be observed, the bond lengths of the corresponding nitro and unsubstituted hydrazones are similar. The calculated heats of formation suggest that the studied compounds prefer the enolic form *a*. It can also be seen that C–C bond lengths in the quinoid ring of the keto form *b* are alternating between short and long values, suggesting that this ring loses aromaticity in going from *a* to *b*. Meanwhile, the adjacent ring in $2,4(NO_2)_2PHNH$ becomes more aromatic as the proton is transferred from the oxygen to the nitrogen. Although this aromaticity transfer may favour form *b*, the results suggest that this effect is not strong enough to shift the equilibrium position. Obviously, the aromaticity transfer is absent in $2,4(NO_2)_2PHPH$, which therefore is forced to exist in form *a*.

3.2. Deprotonation constants

Due to the low aqueous solubility of both $2,4(NO_2)_2PHPH$ and $2,4(NO_2)_2PHNH$, their acidity constants were spectrophotometrically evaluated in 70% v/v dioxane–water solutions. The pK_a values obtained at 20°C and $\mu = 0.10$ M were: 11.1 ± 0.1 and 10.4 ± 0.1 for $2,4(NO_2)_2PHPH$ and $2,4(NO_2)_2PHNH$, respectively. Fig. 1 shows the absorbance spectra of $2,4(NO_2)_2PHPH$ at different pH values. As shown in this picture, the maximum at 393 nm detected at acid pH (typical of the enolic structure for the protonated compound) shifts towards a longer wavelength (470 nm) at high pH. The presence of an isosbestic point at 425 nm indicates an equilibrium between two absorbent species (the protonated and deprotonated ones). In the case of

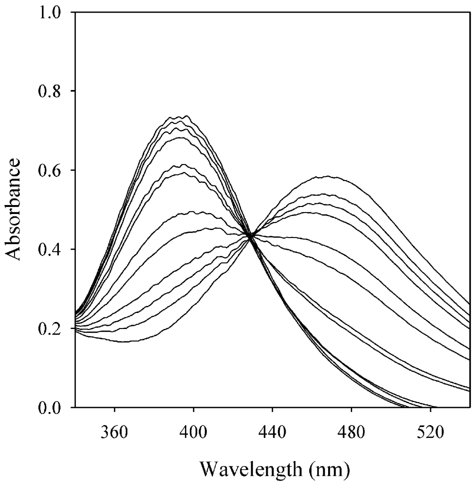

Fig. 1. Absorbance spectra at different pH values of $2,4(NO_2)_2PHPH$ in 70% v/v dioxane–water; initial $C_{2,4(NO_2)_2PHPH} = 2.84 \times 10^{-5}$ M, $\mu = 0.10$ M ($NaNO_3$), $t = 20.0$°C.

$2,4(NO_2)_2PHNH$, when the pH increases, a shift of the absorption maximum (from 415 to 490 nm) is also observed, while the isosbestic point is detected at 450 nm. The behaviour of both hydrazones with increasing pH indicates conversion of the enolic hydroxy groups into the enolate ions, which resemble a keto–hydrazonic anion having a quinoid structure (Scheme 2).

In agreement with these results, PM3 geometry optimisation of both anions yields structures with significant quinoid character (see the bond lengths for the N–N–C–C–O moiety quoted in Table 2). Notice that each anion is in principle able to exist in two different isomeric forms, identified as *A* and *B* in Table 2: they differ in the configuration of the double C(7,9)=N(1) bond. In *A*, N(2) is *trans* with respect to C(7,9), whereas in *B* the configuration is *cis*. As is apparent in Table 2, the heats of formation show that *B* is considerably more stable than *A*. This may conceivably due to the strong hydrogen bond formation $N(2)\text{–}H\cdots O^-$ (see Scheme 2). As was the case with the protonated compounds, the anionic form of $2,4(NO_2)_2PHNH$ is in principle able to suffer aromaticity transfer, in contrast to the $2,4(NO_2)_2PHPH$ anion. According to the C–C bond lengths of the adjacent aromatic ring (intermediate between single and double bond values) it can be concluded that additional stability of form *b* is obtained from this process (Table 2).

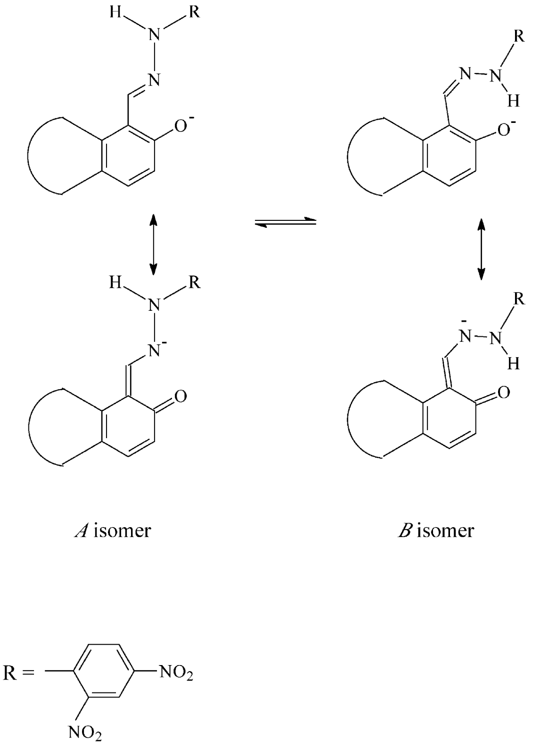

Scheme 2.

3.3. Metal–α-hydroxy hydrazone complexes

Due to significant solubility problems of the metal systems formed by the naphtholic derivatives, only the phenolic ones were analysed. Nevertheless, even these studies required to be performed in dioxane–water solutions. While the potentiometric technique is considered as an accurate method for the obtainment of reliable equilibrium constant values, spectrophotometric measurements are a useful tool when the former cannot be employed, for instance when precipitate is formed at the concentrations required for potentiometric analysis. On the other hand, the spectrophotometric method is limited by the fact that association reactions are not favoured at low concentrations of reagents. In the present work, both methods were applied for the equilibrium constant determinations, and the limitations found are discussed in each case.

Table 2
Relevant PM3 results for the deprotonated compounds (bond lengths are in Å)

Parameter	PHPH		PHNH		2,4(NO$_2$)$_2$PHPH		2,4(NO$_2$)$_2$PHNH	
	A	*B*	*A*	*B*	*A*	*B*	*A*	*B*
ΔH_f^0 (kJ mol^{-1})	66.7	19.2	116.5	76.1	− 69.3	− 116.7	− 19.7	− 56.6
N–N–C–C–C–O portion								
N–N	1.436	1.400	1.429	1.401	1.404	1.395	1.403	1.397
N–C(7,9)	1.316	1.303	1.315	1.304	1.335	1.313	1.338	1.314
C(7,9)–C(1)	1.431	1.450	1.432	1.447	1.407	1.432	1.404	1.430
C(1)–C(2)	1.455	1.443	1.452	1.436	1.460	1.443	1.460	1.438
C(2)–O	1.239	1.261	1.237	1.256	1.234	1.259	1.231	1.255
Aromatic ring bearing the oxygen								
C(2)–C(3)	1.471	1.450	1.480	1.466	1.477	1.457	1.484	1.468
C(3)– C(4)	1.356	1.365	1.344	1.349	1.350	1.359	1.341	1.346
C(4)–C(5)	1.416	1.406			1.425	1.414		
C(5)–C(6)	1.372	1.380			1.361	1.369		
C(6)–C(1)	1.410	1.401			1.425	1.418		
C(4)–C(4a)			1.437	1.431			1.443	1.435
C(4a)–C(8a)			1.420	1.418			1.414	1.413
C(8a)–C(1)			1.422	1.421			1.441	1.438
Adjacent aromatic ring								
C(4a)–C(5)			1.403	1.408			1.402	1.408
C(5)–C(6)			1.379	1.375			1.381	1.376
C(6)–C(7)			1.403	1.407			1.398	1.403
C(7)–C(8)			1.373	1.370			1.378	1.374
C(8)–C(8a)			1.424	1.426			1.416	1.421

3.3.1. Metal–PHPH complexes

We have previously studied the complex formation between Cu(II) and PHPH [5]. The results showed that this compound forms cupric chelates with different degrees of deprotonation and presents a metal coordination with the oxygen, nitrogen N(1) and hydroxyl groups. In the present work, the study was extended to two additional divalent ions [Co(II) and Ni(II)] and to trivalent cations [Fe(III) and Al(III)]. However, in our working conditions, no significant complex formation was established with the latter two metals.

The interaction between the studied ligands and a divalent metal ion can be explained through the following global equilibria:

$$M^{2+} + LH \rightleftharpoons [MLH_{-1}] + 2H^{+} \quad (1)$$

$$M^{2+} + LH \rightleftharpoons [MLH_{-2}] + 3H^{+} \quad (2)$$

where LH is the protonated ligand, M^{2+} is the studied metal and the negative stoichiometric coefficient under the H represents the number of protons displaced upon complexation (in addition to the ligand proton), which could arise from coordinated water molecules. Although both 1:1 and 1:2 metal–ligand stoichiometric ratios were evaluated, only 1:1 complexes were found. Fig. 2A shows the potentiometric profile for the Co(II)–PHPH system. A precipitate was observed for about pH 7.3, yet in the soluble region the $[CoLH_{-1}]$ complex was detected with a maximum concentration of 16% with respect to the total analytical metal ion concentration. The obtained equilibrium constant value is shown in Table 3. The presence of a solid phase in alkaline medium prevented the evaluation of more deprotonated complexes. Since the concentrations of free cobalt(II) ion and OH^{-} before solid detection were insufficient to produce $Co(OH)_2$, the solid phase was attributed to the precipitation of the neutral $[CoLH_{-1}]$ complex. The Co(II)–PHPH system was also spectrophotometrically investigated (Fig. 3). In this case,

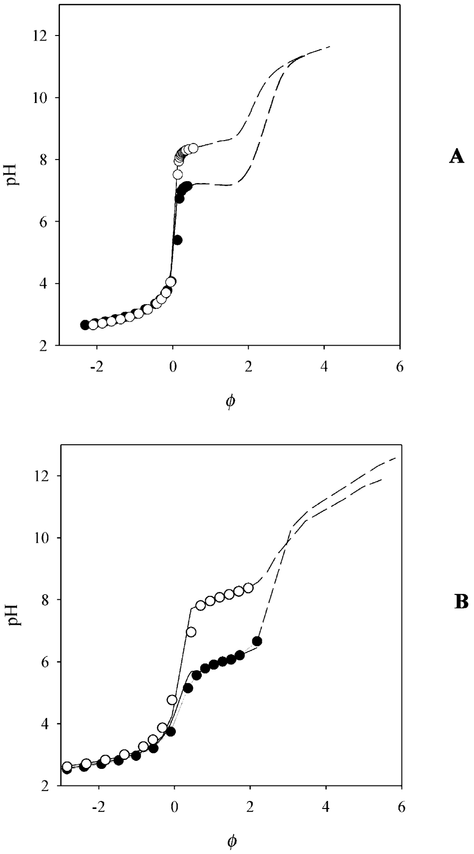

Fig. 2. (A) Potentiometric equilibrium curves in 30% dioxane–water solvent for (●) Co(II)–PHPH ($C_{\mathrm{Co(II)}} = 9.60 \times 10^{-4}$ M, $C_{\mathrm{PHPH}} = 9.90 \times 10^{-4}$ M) and (○) Ni(II)–PHPH ($C_{\mathrm{Ni(II)}} = C_{\mathrm{PHPH}} = 1.06 \times 10^{-3}$ M). (B) Potentiometric equilibrium curves in 70% dioxane–water solvent for (●) Cu(II)–2,4(NO$_2$)$_2$PHPH ($C_{\mathrm{Cu(II)}} = 9.71 \times 10^{-4}$ M, $C_{2,4(\mathrm{NO_2})_2\mathrm{PHPH}} = 1.03 \times 10^{-3}$ M) and (○) Ni(II)–2,4(NO$_2$)$_2$PHPH ($C_{\mathrm{Ni(II)}} = 8.37 \times 10^{-4}$ M, $C_{2,4(\mathrm{NO2})_2\mathrm{PHPH}} = 9.38 \times 10^{-4}$ M); $\mu - 0.10$ M (NaNO$_3$); $t = 20.0$°C; Φ is the moles of base per mole of ligand or metal. The solid lines corresponding to calculated pH values and precipitate is indicated by dashed lines.

since more diluted solutions were used, precipitation was not detected and the computational processing of the data indicated the presence of both [CoLH$_{-1}$] and [CoLH$_{-2}$]$^-$ chelates. The more deprotonated complex was detected above pH 8 and reached a concentration of ca. 100% at pH > 10. The values of the formation constants are displayed in Table 3 and, as can be appreciated, the one corresponding to the neutral species is similar to that found using the potentiometric method.

Table 3
Log of equilibrium constant values for metal–PHPH complexes, $t = 20.0°C$, $\mu = 0.10$ M (NaNO$_3$), 30–70% v/v dioxane–water (charges are omitted)

Quotient	Potentiometry	Spectrophotometry
Co(II)		
[CoLH$_{-1}$][H]^2/[Co][LH]	− 11.77 ± 0.02	− 11.6 ± 0.1
[CoLH$_{-2}$][H]^3/[Co][LH]		− 21.7 ± 0.1
	$\sigma_{\mathrm{fit}} = 0.018$	$\sigma_{\mathrm{fit}} = 0.013$
Ni(II)		
[NiLH$_{-1}$][H]^2/[Ni][LH]	− 14.21 ± 0.02	− 13.9 ± 0.1
[NiLH$_{-2}$][H]^3/[Ni][LH]		− 25.3 ± 0.1
	$\sigma_{\mathrm{fit}} = 0.022$	$\sigma_{\mathrm{fit}} = 0.013$
Cu(II)[a]		
[CuLH$_{-1}$][H]^2/[Cu][LH]		− 7.5
[CuLH$_{-2}$][H]^3/[Cu][LH]		− 17.5

[a] From Ref. [5].

The potentiometric behaviour of the Ni(II)–PHPH system is similar to that for the Co(II) one (Fig. 2), with the [NiLH$_{-1}$] complex also detected in the soluble region. Although the yellow–green precipitate formed is ascribed to the neutral complex, the relevant product of free concentrations [Ni^{2+}] × [OH$^-$]^2 before precipitation is close to the K_{sp} of Ni(OH)$_2$, and thus coprecipitation of this species cannot be discarded. In the Ni(II)–PHPH spectrophotometric studies, no solid

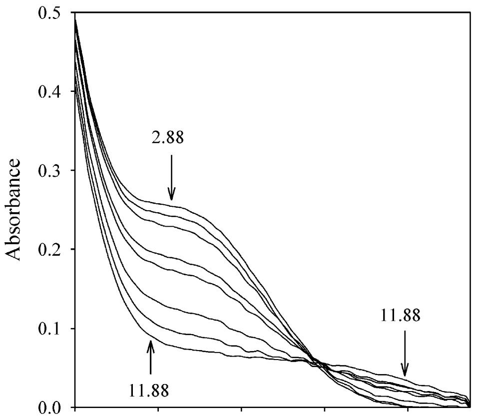

Fig. 3. Absorbance spectra at different pH values of the Co(II)–PHPH system in 30% v/v dioxane–water; initial $C_{\mathrm{Co(II)}} = C_{\mathrm{PHPH}} = 2.04 \times 10^{-5}$ M, $\mu = 0.10$ M (NaNO$_3$), $t = 20.0$°C. For clarity only some spectra are illustrated.

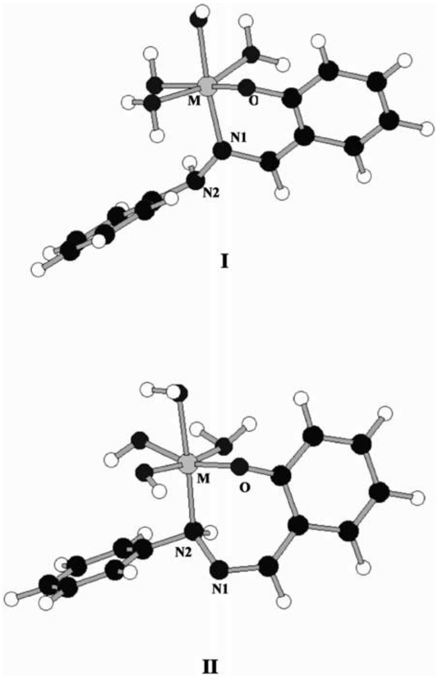

Scheme 3.

formation was observed, and the results were explained on the basis of the presence of both $[NiLH_{-1}]$ and $[NiLH_{-2}]^-$ complexes. The equilibrium constant values obtained for these complexes (Table 3) can be compared with those of Cu(II) and Co(II) systems. The fact that the equilibrium constants of the Cu(II) complexes supports larger the conclusion that this metal ion interacts strongly with the type of studied donor groups. A similar conclusion was obtained with related azocompound systems [21].

Table 4
Heats of reaction (ΔH^0) for metal–PHPH and metal–2,4$(NO_2)_2$PHPH complexes (I is the arrangement with six-membered ring, II is the arrangement with seven-membered ring; values in kJ mol^{-1})

	PHPH	2,4$(NO_2)_2$PHPH	
	I	I	II
Co(II)	− 230.5[a] − 400.5[b]		− 177.6[a] − 376.8[b]
Ni(II)	− 273.4	− 232.8	
Cu(II)	− 89.4	− 51.3	

[a] High spin.
[b] Low spin.

As was indicated in a previous report [5], both *A* and *B* anionic forms of α-hydroxy hydrazones may coordinate the metal ion. In the first case, a six-membered ring complex can be formed with a coordination involving the oxygen and the nitrogen N(1) (arrangement type I). In the second case, the metal coordination may involve the oxygen atom and the lone pair electrons of N(2), after proper rotation about the N(1)–N(2) single bond (arrangement type II). Scheme 3 illustrates both type of arrangements. In both cases, either tetra or hexacoordinated geometries can be proposed, with the other binding positions fulfilled with hydroxyl groups and water molecules. For comparing the relative stabilities of the chelates involving the proposed arrangements, semiempirical calculations using PM3 were performed. In all cases, the heat of reaction corresponding to the following transformation was computed:

$$[MLH_{-2}]^- \text{ (tetracoordinated)} + 2H_2O \rightleftharpoons [MLH_{-2}]^- \text{ (hexacoordinated)} \quad (3)$$

The results are collected in Table 4, including both *A* and *B* isomeric forms of the ligand. As can bee seen, despite the higher steric compression introduced by the additional water molecules, the hexacoordinated species (arrangement I) are more stable. Also, among the Co(II) complexes, those of low spin are favoured.

3.3.2. Metal–2,4$(NO_2)_2$PHPH complexes

Because the metal systems formed by this ligand resulted in low solubilities, both potentiometric and spectrophotometric evaluations were performed in mixtures of 70% v/v dioxane–water.

The potentiometric equilibrium profile of pH vs Φ (Φ: mol of base added per mol of ligand or metal) for the 1:1 Cu(II)–2,4$(NO_2)_2$PHPH system is shown in Fig. 2B. Above pH ~ 6.5, a fine precipitate is observed, which then dissolves at high pH. Nevertheless, the data corresponding to pH > 6.5 were not employed in equilibrium computations. The curve was satisfactorily fitted by considering both $[CuLH_{-1}]$ and $[CuLH_{-2}]^-$ species (the latter are present with concentrations higher than 40% before precipitations occurs). The appearance of a solid phase is ascribed to the neutral $[CuLH_{-1}]$ complex

Table 5
Log of equilibrium constant values for metal–2,4$(NO_2)_2$PHPH complexes, $t = 20.0°C$, $\mu = 0.10$ M $(NaNO_3)$, 70–30% v/v dioxane–water (charges are omitted)

Quotient	Potentiometry	Spectrophotometry
Co(II)		
$[CoLH_{-1}][H]^2/[Co][LH]$		-12.7 ± 0.1
$[CoLH_{-2}][H]^3/[Co][LH]$		-22.8 ± 0.1
		$\sigma_{fit} = 0.011$
Ni(II)		
$[NiLH_{-1}][H]^2/[Ni][LH]$	-13.0 ± 0.1	
$[NiLH_{-2}][H]^3/[Ni][LH]$	-21.3 ± 0.1	
	$\sigma_{fit} = 0.037$	
Cu(II)		
$[CuLH_{-1}][H]^2/[Cu][LH]$	-8.68 ± 0.05	
$[CuLH_{-2}][H]^3/[Cu][LH]$	-15.1 ± 0.1	
	$\sigma_{fit} = 0.032$	

precipitation, while the dissolution of this solid is attributed to increasing concentrations of the anionic $[CuLH_{-2}]^-$ complex. The stoichiometries of the species found (Table 5) are similar to those for the PHPH systems. However, since the values were obtained in different solvent media, they cannot be strictly compared. The spectrophotometric curves at different values of pH for the 1:1 Cu(II)–2,4$(NO_2)_2$PHPH system exhibit a similar behaviour to that of the ligand alone. This can be ascribed either to low concentrations of the complexes in the experimental conditions or to the similarity of the extinction coefficients for the complexes and the deprotonated ligand. These facts do not allow the spectrophotometrical determination of the equilibrium constants without incurring in large errors in the calculated values.

Due to the insolubility of the Co(II)–2,4$(NO_2)_2$PHPH system in almost all of the potentiometric curve, the complexes formed could not be studied by this method. However, from spectrophotometric titrations, the species $[CoLH_{-1}]$ and $[CoLH_{-2}]^-$ were found and their constant values are shown in Table 5.

Finally, in the soluble region of the Ni(II)–2,4$(NO_2)_2$PHPH potentiometric curve (Fig. 2B), the $[NiLH_{-1}]$ and $[NiLH_{-2}]^-$ species were found. The electronic spectral patterns at different pH values of the Ni(II)–2,4$(NO_2)_2$PHPH system are similar to those found in the cupric system, and therefore the corresponding constant values could not be spectrophotometrically determined for similar reasons.

Through the equilibrium constant values shown in Table 5, it can be seen that the cupric complexes are more stable than the analogous Co(II) and Ni(II) ones.

In order to optimise the geometries of these complexes and to calculate the heats of formation of the structures, semiempirical calculations using PM3 were performed (Table 4). The obtained results indicate that while hexacoordinated structures with six-membered rings are more stable for both Cu(II) and Ni(II) complexes, the hexacoordinated structure with a seven-membered ring is favoured for the Co(II) complex. Also, it can be observed that among the Co(II) complexes, those of low spin are more stable.

Acknowledgements

Financial support from the University of Rosario, CONICET, Fundación Antorchas and Agencia Nacional de Promoción Científica y Tecnológica (Project PICT99 No 06-06078) is gratefully acknowledged.

References

[1] J.K. Sears, J.R. Darby, The Technology of Plasticizers, Wiley, New York, 1982.
[2] E. Massarani, D. Nardi, A. Tajana, L. Degen, J. Med. Chem. 14 (1971) 633.
[3] J.D. Ranford, J.J. Vittal, Y.M. Wang, Inorg. Chem. 37 (1998) 1226.
[4] J.A. Arancibia, A.C. Olivieri, G.M. Escandar, J. Mol. Struct. 522 (2000) 233.
[5] G.N. Ledesma, M. Gonzalez Sierra, G.M. Escandar, Polyhedron 17 (1998) 1517.
[6] G.A. Ibañez, A.C. Olivieri, G.M. Escandar, J. Chem. Soc. Faraday Trans. 93 (1997) 545.
[7] G.N. Ledesma, G.A. Ibañez, G.M. Escandar, A.C. Olivieri, J. Mol. Struct. 415 (1997) 115.
[8] G.A. Ibáñez, A.C. Olivieri, G.M. Escandar, J. Mol. Struct. 435 (1997) 199.
[9] G. Schwanzerbach, Complexometric Titrations, Interscience, New York, 1960.
[10] F.J. Rossotti, H.J. Rossotti, J. Chem. Ed. 42 (1965) 375.
[11] A.I. Vogel, Practical Organic Chemistry, Longmans, London, 1961 (p. 722).
[12] J.J. Steward, J. Comput. Chem. 12 (1991) 320.

[13] L.G. Van Uiter, C.G. Hass, J. Am. Chem. Soc. 75 (1953) 451.

[14] R.J. Motekaitis, A.E. Martell, Inorg. Chem. 27 (1988) 2718.

[15] C.F. Baes Jr., R.E. Mesmer, The Hydrolysis of Cations, R.E. Krieger, Malabar, FL, 1986.

[16] A.E. Martell, R.J. Motekaitis, The Determination and Use of Stability Constants, 2nd ed., VHC, New York, 1992 (p. 143).

[17] J.L. Beltrán, R. Codony, M.D. Prat, Anal. Chim. Acta 276 (1993) 441.

[18] S.H. Alarcón, A.C. Olivieri, R.M. Cravero, G. Labadie, M. González-Sierra, Tetrahedron 51 (1995) 4619.

[19] S.H. Alarcón, A.C. Olivieri, R.M. Cravero, G. Labadie, J. Phys. Org. Chem. 8 (1995) 713.

[20] S.H. Alarcón, M. González-Sierra, A.C. Olivieri, J. Chem. Soc. Perkin Trans. 2 (1994) 1067.

[21] G.A. Ibañez, G.M. Escandar, Polyhedron 17 (1998) 4433.